Channel Model for Tyre Pressure Monitoring Systems (TPMS)

Gregor Lasser and Christoph F. Mecklenbräuker*
Vienna University of Technology
Institute of Communications and Radio-Frequency Engineering
Gusshausstrasse 25/389, 1040 Vienna, Austria
Email: gregor.lasser@nt.tuwien.ac.at

*Christian Doppler Laboratory for Wireless Technologies for Sustainable Mobility

***Abstract*—Tyre pressure monitoring systems rely on radio transmissions to transfer measurement data from the sensors to the vehicle body. These systems operate on a propagation channel which is time variant and introduces Doppler shifts due to vehicle movements. In the following paper we investigate these effects. First we propose, develop and characterise a channel model for TPMS, which is comprised of a deterministic and a stochastic component. In a second part channel simulations with an arbitrary vehicle model are presented to gain insight to the behaviour of TPMS channels. Finally an example out of a series of static channel measurements is shown.**

I. Introduction

Tyre pressure monitoring is currently seen as a key technology to enhance vehicular comfort and safety standards and enable fuel consumption reduction by maintaining optimum tyre inflation. This attitude is also reflected in the legislation of some states, which made TPMS mandatory for new vehicles. Most direct TPM systems use battery powered sensor units in each wheel and a centralised onboard unit (OU) with at least one antenna for reception of the wheel unit (WU) signals. The bulky nature of the WU battery leads to sensor units that are mounted at the rim and often use the valve's protruding part as antenna. To gain new sensor data like tyre tread vibration, vertical load, tyre contact area, and radio frequency identification (RFID) functionality the sensor unit has to be moved to the tyre itself. This new mounting position requires a light-weight WU, so it should be battery-less. To power those advanced tyre monitoring systems (ATMS), the electromagnetic field of the OU could be used like in RFID systems, so radio propagation should also be analysed for that purpose.

As was already noted in [1], that there is a strong demand for intravehicular channel models that capture "the propagation and channel impairments to which the technology is sensitive". The focus of many publications in the TPMS field is on WU and OU antenna design and simulation techniques [2] and channel loss simulations [2], [3] of conventional TPMS. In [4] a geometry based deterministic model was used to derive the Doppler shift for line of sight situations. In this contribution, we propose, develop, and characterise a narrowband radio channel model for TPMS and ATMS mounted in-situ. The model includes near-field and far-field effects. This section is followed by the description of channel simulations of an advanced tyre monitoring system operating in the 868 MHz range and their results for different WU antenna mounting positions.

This work has been funded by Infineon Technologies Austria AG and the Christian Doppler Laboratory for wireless technologies for sustainable mobility.The financial support by the Federal Ministry of Economy, Family and Youth and the National Foundation for Research, Technology and Development is gratefully acknowledged.

II. Channel Model

Radio channels generally exhibit time and frequency dispersion. However, if the symbol duration of the data being transmitted over the channel is very long compared to the delay differences of the various signal components, the time dispersion in such a channel is so small that it can be ignored. In this case the channel is also uniform in the spectral domain and therefore called flat.

The channel is considered flat, if the maximum delay spread $\Delta\tau$ is much smaller than the symbol duration T_S. For our analysis we choose the highest data rate of the popular EPCglobal RFID standard [5, p. 33] of $640\,\mathrm{kHz}$ which corresponds to a symbol duration of $1.5625\,\mu\mathrm{s}$. If we demand the delay spread to be at least ten times smaller, we get a maximum allowed electrical length difference of $46.84\,\mathrm{m}$ for the longest and shortest occurring propagation path. We consider the magnitudes of scattering components from objects being more then $23\,\mathrm{m}$ away as insignificant and therefore state that the flat fading condition is satisfied for TPMS channels.

A. Uplink

The uplink-channel is modelled as a multiple input, single output channel. One OU with a single antenna receives the signals from all WUs, which also have a single antenna. In the case of a regular vehicle, there are four tyres, so with the OU as receiver, the channel is represented by the sum of four individual transmission paths from each WU to the OU. As was argued before these individual channels are narrowband channels and therefore their time-varying impulse responses $\hat{h}_i(t,\tau)$ reduce to a delta function multiplied by a complex time-varying factor $\hat{h}_i(t)$ [6, p. 119].

To model the influence of the channel we split $\hat{h}_i(t)$ in a deterministic and a stochastic component and introduce an additive, white and Gaussian receiver noise component $n(t)$. The deterministic component $h_i\big(\varphi(t), \Theta(t)\big)$ is dependent on the wheel rotational angle φ and on the steering angle Θ, which are both a function of time. The motion of the vehicle will introduce vibrations of vehicle and wheels and alterations of the road surface underneath the vehicle. Changes in the channel coefficients due to these effects are modelled via the stochastic component $\tilde{h}_i(t)$. With this nomenclature the received signal $r_0(t)$ at the OU is the sum over products of the four individual OU-WU channels and the corresponding transmit signals $s_i(t)$ plus noise:

$$r_0(t) = \sum_{i=1}^{4} \Big[h_i\big(\varphi(t), \Theta(t)\big) + \tilde{h}_i(t) \Big] s_i(t) + n(t). \quad (1)$$

For geometrical reasons it is clear, that $h_i(\varphi, \Theta)$ is a 2π periodical function of φ and therefore can be decomposed as a Fourier series:

$$h_i(\varphi, \Theta) = \sum_{m=-\infty}^{\infty} c_{i,m}(\Theta) e^{jm\varphi}, \quad (2)$$

with

$$c_{i,m}(\Theta) = \frac{1}{2\pi} \int_0^{2\pi} h_i(\varphi, \Theta) e^{-jm\varphi} d\varphi. \quad (3)$$

Note that this Fourier series is not defined in time, but in the rotational angle instead. The reason for choosing this approach is the benefit of time independence and therefore speed independence of the channel model parameters. For analysis at a certain vehicular speed v or tyre angular speed ω the corresponding channel parameters $h_i\big(t, \Theta(t)\big)$ can be easily calculated by inserting

$$\varphi = \varphi_0 + \omega t = \varphi_0 + \frac{v}{d\pi} t, \quad (4)$$

where d is the tyre's diameter and φ_0 is the rotational angle at $t = 0$.

B. Downlink

The downlink channel from OU to a specified WU is very similar to the uplink channel which was represented in (1). When we consider the receiving WU numbered i, it's received equivalent baseband signal $r_i(t)$ can be written as

$$\begin{aligned} r_i(t) = &\Big[h_i\big(\varphi(t), \Theta(t)\big) + \tilde{h}_i(t) \Big] s_0(t) \\ &+ \sum_{j=1, j\neq i}^{4} \Big[h_{i,j}\big(\varphi_i(t), \varphi_j(t), \Theta(t)\big) + \tilde{h}_{i,j}(t) \Big] s_j(t) \\ &+ n_i(t). \end{aligned} \quad (5)$$

The first term in (5) represents the desired received equivalent baseband broadcast signal originating from the OU $s_0(t)$. Interference from other WUs is captured in the second term. The transmitted signals from the other WUs $s_j(t)$ are affected by individual channels between the observed and the other tyres corresponding to the channel coefficients $h_{i,j}\big(\varphi_i, \varphi_j, \Theta\big)$ and the associated stochastic parts $\tilde{h}_{i,j}(t)$. Finally, the third term reflects the noise component generated in the OU receiver.

The necessity to analyse the second term depends on the transmission protocols used by the tyre monitoring system. For solutions that guarantee that the slaves (OUs) do not transmit during master (WU) transmissions, like in popular RFID solutions [5], the second term in (5) can be omitted.

C. Truncation of Fourier Series

When we recapitulate the structure of the downlink channel model (5) with a deterministic component $h_i(\varphi(t), \Theta(t))$ and a stochastic component $\tilde{h}_i(t)$ a further possibility of simplification is becoming obvious. The sum in (2) can be limited to some significant components. For practical channels those significant $c_{i,m}$ are grouped around the lower frequencies, so the channel coefficient can be written as a sum over $2M + 1$ components

$$h_i(\varphi, \Theta) = \sum_{m=-M}^{M} \Big[c_{i,m}(\Theta) e^{jm\varphi} \Big] + \epsilon_{i,M}(\varphi, \Theta), \quad (6)$$

and a remainder term $\epsilon_{i,M}(\varphi, \Theta)$ that contains the higher frequency components. If this term is omitted in favour of a simplified channel representation and M is chosen adequately, we get a filtered channel model that is comparable to the full channel representation. It can be argued that this simplification captures only some part of the channels transferred power for the sake of a simpler representation. Due to the presence of a stochastic channel component, the impact of this parameter reduction on the overall channel $\hat{h}_i(t)$ is negligible if the power of the omitted spectral components is much smaller than the power spectral density of the stochastic component in that region.

The same idea can also be applied on the downlink channel model to simplify both deterministic components $h_i\big(\varphi(t), \Theta(t)\big)$ and $h_{i,j}\big(\varphi_i(t), \varphi_j(t), \Theta(t)\big)$.

D. Doppler Shift

To evaluate the Doppler shift introduced by the moving wheels, we have to explicitly show the time dependency of $h_i(\varphi, \Theta)$ by inserting (4) into (2).

$$h_i(t, \Theta) = \sum_{m=-\infty}^{\infty} c_{i,m}(\Theta) \Big(e^{jm\varphi_0} \cdot e^{jm\frac{v}{d\pi}t} \Big) \quad (7)$$

To show the Doppler effect, we calculate the deterministic channel output $r_d(t)$ by inserting a sinewave with frequency f_0

$$\begin{aligned} r_d(t) &= h_i(t, \Theta) s(t) = h_i(t, \Theta) e^{j2\pi f_0 t} \\ &= \sum_{m=-\infty}^{\infty} c_{i,m}(\Theta) \Big(e^{jm\varphi_0} \cdot e^{j2\pi(\frac{mv}{2d\pi^2} + f_0)t} \Big). \end{aligned} \quad (8)$$

So the output signal is a phase and amplitude weighted sum of sinewaves with frequencies f_m:

$$f_m = m\frac{v}{2d\pi^2} + f_0 = mf_D + f_0, \quad (9)$$

where f_D is the Doppler effect's fundamental frequency. For the simplified channel represented by $2M + 1$ Fourier components, as introduced in (6), we can calculate the Doppler bandwidth $B_D = 2M \cdot f_D$.

If we consider a vehicle with tyre dimension 205/55 R16 and a driving speed of $200\,\mathrm{km/h}$ and a channel represented by $M = 16$ frequencies we get a Doppler effect's fundamental frequency f_D of $4.421\,\mathrm{Hz}$ and a Doppler bandwidth B_D of $141.5\,\mathrm{Hz}$.

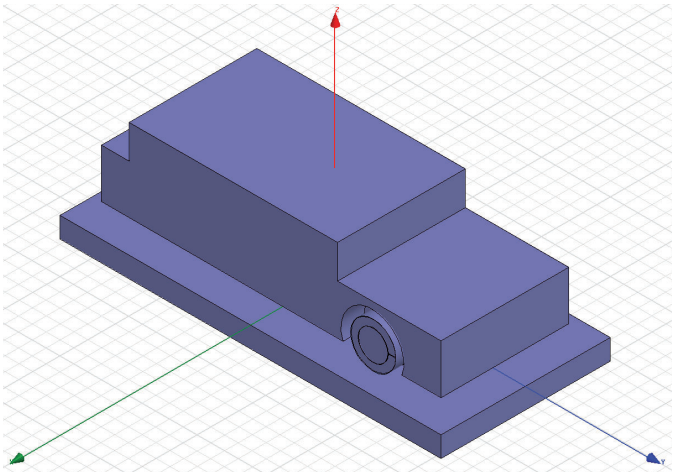

Fig. 1. Simulation model implemented in HFSS.

III. Simulations

To gather numerical results for the deterministic channel component, electromagnetic field simulations in HFSS from Ansoft were carried out. The influence of the changing antenna environment and the relatively small dimensions of the underlying geometry favor the field simulation approach to other propagation channel simulation types like ray tracing.

A. Setup

Fig. 1 shows the very simplified model of a vehicle, which was used for electromagnetic field simulations. The vehicle body is represented by a solid block of steel with cut-outs for the single wheelhouse and motor and luggage compartments. Most of the simulations deal with the analysis of the channel coefficient h_1 from the front right wheel to the onboard unit, so only one wheel is modelled for those cases.

To properly capture proximity effects, special care needs to be taken when modelling the antenna environment. Based on previous work [7], mounting the WU antenna on the tyre's sidewall was found to be the most promising approach, because of the negative influence of the steel belt present on the tread. To keep the simulation model simple, the whole tyre was drawn as a homogeneous piece of rubber, where the electrical parameters of the rubber were chosen to match the equivalent of the combined sidewall rubber mixtures. For the chosen tyre these values are $\tan(\delta) = 0.11$ for the dielectric loss tangent and $\varepsilon_r = 5.5$ for the relative permittivity [8]. Fig. 2a depicts a detail of the vehicle model with highlighted

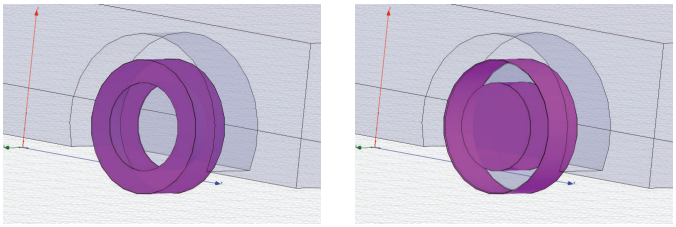

(a) (b)

Fig. 2. Detail of the simulation model implemented in HFSS: tyre rubber parts (a), steel belt and rim (b)

tyre rubber. The tyre's steel belt was represented by a thin solid steel band covering the outside of the rubber tyre part explained before. This steel belt equivalent and the rim which was modelled as a steel cylinder are shown in Fig. 2b.

A dipole was used in the simulation model for the WU antenna, which was mounted in the middle of the tyre's sidewall. Four different mounting orientations were analysed, where this number results from the combination of two parameters: Parallel and orthogonal to the tyre tread and mounted at the inner and outer sidewall of the tyre. For the reader antenna, a monopole was used, which position was kept fixed at the vehicle's bottom plate centre for all simulations. The monopole element of quarter wavelength dimension and the conducting bottom plate of the vehicle form a ground-plane antenna.

B. Results

To evaluate the influence of the road surface, two types of simulation models were used. While the first one does not contain any structures to emulate the road, the second type uses a cuboid of $30\,\mathrm{cm}$ thickness with constant, homogenous and isotropic material parameters. Values of $\tan(\delta) = 0.021$ for the dielectric loss tangent and $\varepsilon_r = 5$ for the relative permittivity were chosen to mimic the road surface.

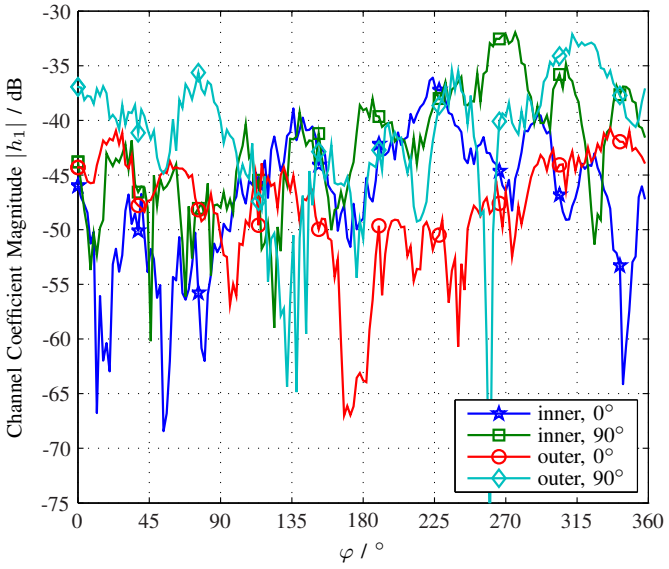

Fig. 3. Simulated channel coefficient $h_1(\varphi, 0)$ for different antenna positions.

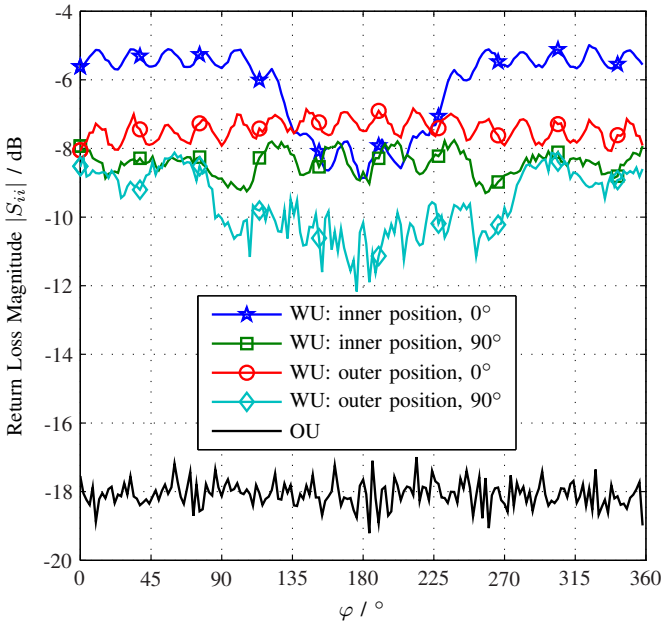

Fig. 4. Return loss of WU and OU antennas.

1) Model without road surface: In Fig. 3 the absolute value of the channel coefficient $h_1(\varphi, 0)$ is plotted over the rotational angle φ for different antenna positions. Zero degrees correspond to the WU antenna being at the topmost position. The influence of the antenna orientation on the average channel losses is quite small, due to the rich multipath propagation environment. For the same reason, a positive effect in the $180°$ region, which could be considered due to the unobstructed quasi line of sight condition between WU and OU antenna, is inexistent.

There is close electromagnetic coupling between the rotating wheel with its sensor antenna and the vehicle body. To investigate the influence of this coupling the antenna return losses for different mounted WU antennas is plotted in Fig. 4. For the cases where the WU antenna is oriented parallel to the tyre tread, the ringing clearly identifies a dominant higher frequency component. The expected change in the return loss in an region centred around $180°$ due to the absence of the wheelhouse is also present. For comparison the return loss of the OU antenna is plotted to see the effect of the numerical simulation errors.

To investigate the practical feasibility of the parameter reduction introduced in (6), the simulated channel is plotted in the Fourier domain. Fig. 5 shows the magnitudes of the Fourier components for the case of a WU antenna mounted on the inner sidewall parallel to the tread. The spectrum of the corresponding antenna return loss is plotted in Fig. 6. It is obvious that most of the channel power is concentrated in a small band around zero, which indicates that spectral reduction introduced in (6) is indeed feasible. As a summation limit $M = 16$ was chosen, which corresponds to the last peaks in the antenna return loss magnitude spectrum, or rather the ringing visible in Fig. 4. This simplification captures $98.4\,\%$ of the channel's transferred power but only uses $18.3\,\%$ of the

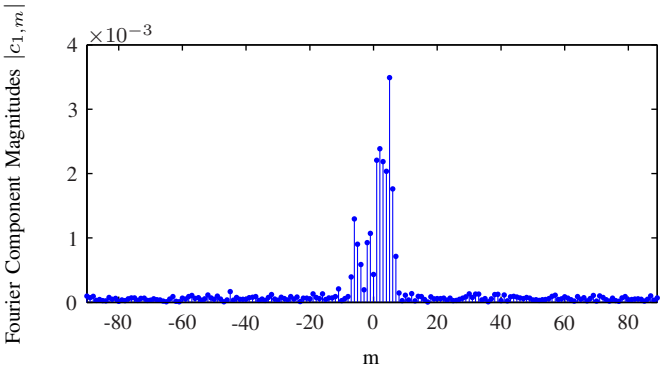

Fig. 5. Fourier components $c_{1,m}$ for a inner parallel mounted antenna.

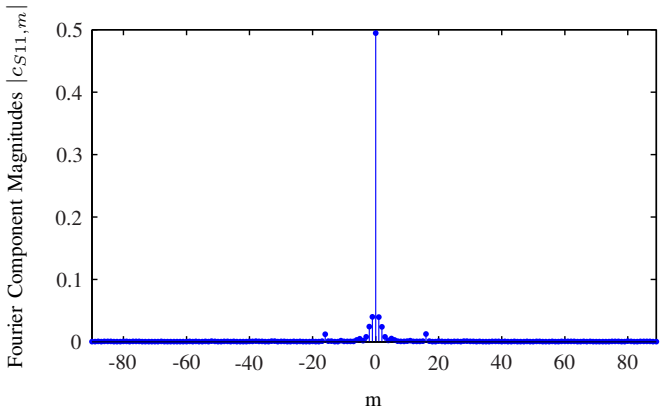

Fig. 6. Fourier components $c_{S11,m}$ for a inner parallel mounted antenna.

180 Fourier components obtained from the simulation results.

2) Model with road surface: The application of a simple road surface structure in the simulation model introduces a large scattering object in close distance to both involved antennas. This leads to more scattering and fading effects and more high frequency components in the deterministic channel parameter. As an example, Fig. 7 shows the spectrum of an outer mounted antenna oriented parallel to the tread. When compared to Fig. 5 and the simulations without road surface, the basic structure of few strong components centered around zero remains the same, but the higher frequency components become more dominant. Still, $92\,\%$ of the channel's transferred power is captured when using a simplified representation with $M = 16$, as before.

For the same sensor antenna orientation, Fig. 8 compares this filtered channel response to the filtered channel between the front wheel sensors. In this simulation both front wheels were assumed to run completely aligned, so that the abscissa labeling is valid for both front WUs. For this mounting position the channel loss between the front wheel sensors is for many cases about $20\,\mathrm{dB}$ lower than the loss between one WU and the onboard unit. This is potentially harmful in the downlink, especially to systems that do not employ a strict master-slave scheme.

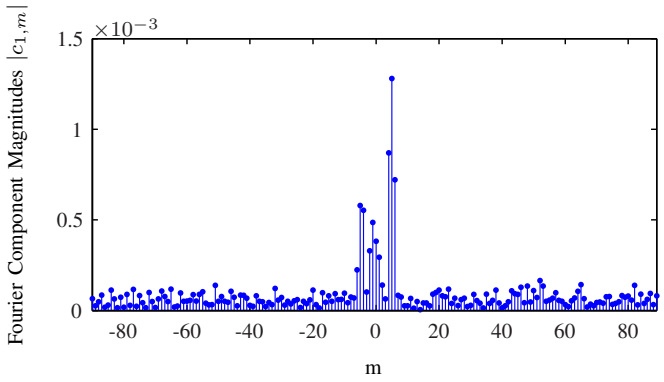

Fig. 7. Fourier components $c_{1,m}$ for an outer parallel mounted antenna.

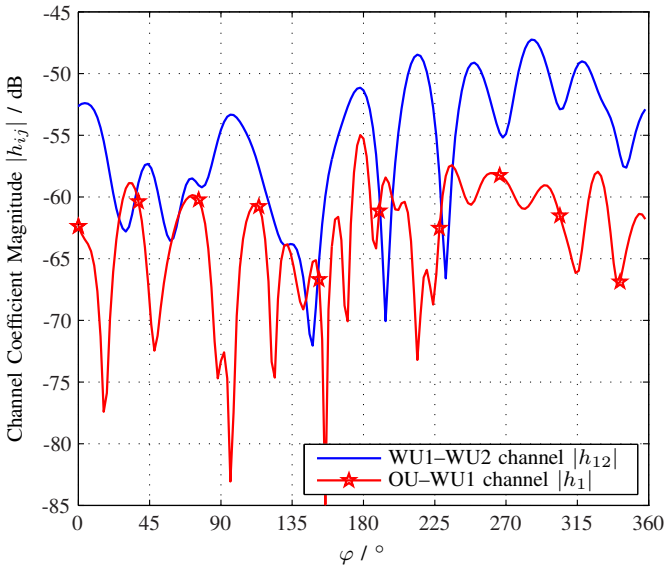

Fig. 8. Simulated WU-OU and WU-WU channel responses for outer parallel mounted antennas.

IV. Static Channel Measurements

Simulations, especially where complex electromagnetic scenarios like a vehicle body are radically simplified for the simulation model are error prone. For that reason the aim of the presented simulations was not to obtain quantitative correct results for a specific vehicle model, but instead gain insight to the general behavior of ATMS channels. To validate these general trends but also obtain results for a specific vehicle, measurements with a Golf V were carried out [9].

Fig. 9 presents the measurement results of the channel response at 866 MHz between an inner mounted orthogonal oriented WU dipole antenna, and a dual-band ground-plane OU antenna mounted on the vehicles bottom plate. In this plot the channel response for three different steering angles is compared, whereas $\Theta = -25°$ corresponds to one complete turn of the steering wheel to the left. The average losses approximately stay the same, but the run of the curve is changed due to the alteration of the rotation plane and the wheelhouse-wheel distances.

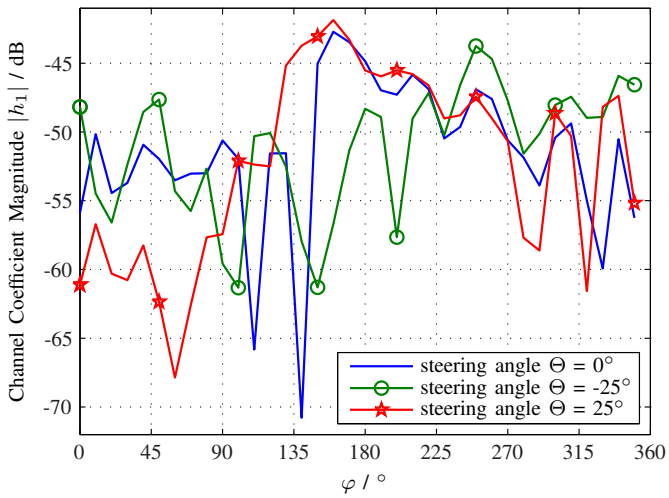

Fig. 9. Measured channel coefficient $h_1(\varphi, \Theta)$ for an inner mounted orthogonal antenna for different steering angles.

V. Conclusion

TPM systems operate on a time-variant flat fading channel. We developed a channel model for such systems, whose channel coefficient is split into a deterministic and a stochastic component. A practical method to reduce the complexity of the channel representation was shown, based on this model. Further, we derived the Doppler bandwidth, discussed field simulations and the obtained channel responses for a vehicle model. These simulation results indicate that the parameter reduction technique is feasible, and showed the high dynamic range of the channel losses, which are between 33 dB to 85 dB. Finally, a measurement result was presented to give an example of the dependence of the channel response on the steering angle.

References

[1] D. G. Michelson, J. Chuang, and M. Kicherer, "Requirements for standard radiowave propagation models for vehicular environments," *Vehicular Technology Conference, 2006. VTC 2006-Spring. IEEE 63rd*, vol. 6, pp. 2777–2781, May 2006.

[2] M. Brzeska and G.-A. Chakam, "RF modelling and characterization of a tyre pressure monitoring system," *The Second European Conference on Antennas and Propagation, 2007. EuCAP*, pp. 1–6, Nov 2007.

[3] H. J. Song, H. P. Hsu, R. Wiese, and T. Talty, "Modeling signal strength range of TPMS in automobiles," *Antennas and Propagation Society International Symposium, 2004. IEEE*, vol. 3, pp. 3167 – 3170, June 2004.

[4] Y. Leng, Y. Pan, Q. Li, and S. Liu, "Analysis of electromagnetic wave propagation characteristics in rotating environments," *International Conference on Electronic Packaging Technology & High Density Packaging*, pp. 1–7, July 2008.

[5] EPCglobal, "EPC radio-frequency identity protocols class-1 generation-2 UHF RFID protocol for communications at 860 MHz – 960 MHz version 1.2.0," March 2007.

[6] A. F. Molisch, *Wireless communications*, 1st ed. John Wiley & Sons, LTD, 2005.

[7] J. Grosinger, L. W. Mayer, C. F. Mecklenbräuker, and A. L. Scholtz, "Input impedance measurement of a dipole antenna mounted on a car tire," in *Proc. 2009 International Symposium on Antennas and Propagation*, Bangkok, Thailand, October 2009, pp. 1175–1178.

[8] ——, "Determining the dielectric properties of a car tire for an advanced tire monitoring system," *Vehicular Technology Conference. VTC 2009-Fall. IEEE 70th*, September 2009.

[9] G. Lasser and C. F. Mecklenbräuker, "Dual-band channel measurements for an advanced tyre monitoring system," *Vehicular Technology Conference. VTC 2010-Spring. IEEE 71th*, accepted for publication.